Uniform quantization conditions in the presence of symmetry: The rotational spectrum of SF_6

Jonathan M. Robbins, Stephen C. Creagh, and Robert G. Littlejohn
Department of Physics, University of California, Berkeley, California 94720
(Received 2 January 1990)

Uniform semiclassical quantization conditions are obtained for a one-dimensional Hamiltonian possessing octahedral symmetry. The Hamiltonian describes the rotational dynamics of SF_6, a system in which tunneling plays an important role. Quantization conditions are obtained for each symmetry class. These are shown to agree with previously obtained primitive quantization conditions in the small tunneling limit and to reproduce a characteristic periodicity in the symmetries labels. Quantum and semiclassical eigenvalues are computed numerically. Near the classical separatrix the uniform quantization provides orders of magnitude improvement in accuracy over primitive quantization. Our calculation is based on periodic orbit theory, modified here to include classically forbidden reflections and transmissions, and completes a study undertaken in a previous paper. The methods used may be generalized to other Hamiltonians and symmetry groups.

I. INTRODUCTION

In a semiclassical treatment of tunneling, it is desirable to obtain quantization conditions which are uniform. Uniform quantization conditions remain valid near classical separatrices, where tunneling amplitudes are no longer small. If the system under consideration possesses symmetry, one would also like the quantization conditions to determine the symmetries of the energy levels. The simplest example of a tunneling system with symmetry is the symmetric double well. For this example, uniform quantization conditions accurate both below and above the barrier are well known,[1] and one easily assigns parities based on them. For example, below the barrier the energy levels occur in nearly degenerate doublets. Within a doublet, the lower-energy state is symmetric under reflection, and the higher-energy state is antisymmetric. In this paper we derive analogous uniform quantization conditions for a system whose dynamics has a more complicated topology and a nontrivial symmetry group.

The system we consider is a model for the rotational dynamics of the octahedrally symmetric molecule SF_6. Ultrahigh-resolution spectroscopy has revealed a rich structure in the rotational spectrum of SF_6.[2,3] The gross structure is that of a spherical top, in which rotational energies depend only on the total angular momentum. However, vibration-rotation interactions create nonspherical perturbations in the moment of inertia tensor and introduce fine structure in the spherical top spectrum. Tunneling between equivalent rotational motions produces an even smaller superfine structure within the fine structure. There also exists a remarkable periodicity in the octahedral symmetry labels. The theory underlying the spectrum has been extensively developed,[4-6] most notably by Harter and Patterson,[7-9] who obtain semiclassical quantization conditions in the small tunneling limit. In this limit they obtain an elegant derivation of the periodic sequence of symmetry labels.

The semiclassical quantization of rotational dynamics has been studied by several authors.[10] In particular, Colwell, Handy and Miller, using methods of traditional WKB theory, have obtained uniform quantization conditions for the asymmetric top.[11] It is more difficult to apply these methods to the SF_6 rotational Hamiltonian, because its Hamiltonian is not a sum of kinetic and potential terms, and the topology of the classical dynamics is complicated. Tunneling occurs among six or eight equivalent classical orbits rather than two, as with the asymmetric top and the symmetric double well.

Our derivation is based instead on periodic orbit theory. Periodic orbit theory, as developed by Gutzwiller, Balian and Bloch, and Berry, provides a semiclassically approximate expression for the trace of the quantum-mechanical Green's function in terms of a sum over classical periodic orbits.[12-14] It is an important tool in the study of quantum chaos, i.e., the study of systems whose classical limit is chaotic. Indeed, it is the basis for the only known analytic results concerning the spectra of such systems. Pursuing a different application, several authors have applied periodic orbit theory to tunneling problems.[15-19] Tunneling effects are introduced by including complex as well as real orbits in the sum. A principal advantage of these treatments is their representation independence. Unlike traditional WKB methods, which are usually carried out in the coordinate representation, periodic orbit theory involves only geometrical and topological features of the classical dynamics, and its formulation is coordinate free.

In a previous paper,[20] referred to in what follows as I, we carried out the complex periodic orbit sum for a model Hamiltonian describing the rotational dynamics of SF_6 and obtained semiclassical quantization conditions equivalent to those of Harter and Patterson.[9] Here we

modify the prescription proposed in I. We introduce the WKB barrier reflection and transmission coefficients. This leads to uniform quantization conditions; these depend on the actions of the classically allowed and forbidden orbits, as well as the representations of the generators of the octahedral group. We obtain separate quantization conditions for each symmetry class. From these, we derive the periodic sequence of symmetry labels, and show that it proceeds without interruption through the separatrix. Quantum-mechanical and semiclassical eigenvalues are computed numerically. Near the separatrix, the uniform quantization is one to two orders of magnitude better than previous quantization schemes. The paper is organized as follows. In Sec. II we derive the uniform quantization conditions. Numerical results are presented in Sec. III, and conclusions are given in Sec. IV. Some explicit calculations are presented in the Appendixes.

II. DERIVATION OF QUANTIZATION CONDITIONS

This section is organized as follows. Section II A contains a discussion of the rotational Hamiltonian in the quantum and classical settings. In Sec. II B, the complex periodic orbit sum is carried out, and the uniform quantization conditions are obtained. Several analytical results follow. The small tunneling limit of the uniform quantization conditions is examined in Sec. II C and is shown to be equivalent to the primitive quantization conditions. In Sec. II D we show that the uniform quantization conditions are continuous at the separatrix and may be analytically continued around it. In Sec. II E we derive the periodic sequence of symmetry labels. Throughout this discussion we take $\hbar=1$.

A. The Hecht Hamiltonian

The rotational spectrum of octahedral-symmetric molecules is well described by the Hecht Hamiltonian,[4]

$$H(\mathbf{J})=aJ^2+b(J_x^4+J_y^4+J_z^4-\tfrac{3}{5}J^4) . \tag{1}$$

H is a function of the body-fixed angular momentum operators $\mathbf{J}$ that act on angular momentum states $|jk\rangle$ in the usual way. The first term in Eq. (1) is the rigid-body Hamiltonian for a spherical top. The second term, which breaks the spherical symmetry, describes centrifugal distortions of the moment of inertia tensor due to rotation-vibration coupling. The parameters a and b may be fit to spectroscopic data; for SF_6, $a=0.091\,083\ \mathrm{cm}^{-1}$ and $b=1.81\times10^{-9}\ \mathrm{cm}^{-1}$.[3,21] Thus the effect of the rotation-vibration coupling is small. The Hamiltonian conserves the total angular momentum J^2, so that j is a good quantum number. For given j, the rotational energies are obtained by diagonalizing H in the $(2j+1)$-dimensional subspace spanned by $|jk\rangle$, where $-j\le k\le j$. In this subspace the spherical top term is completely degenerate; it is the centrifugal term which breaks the degeneracy. We observe that H has octahedral symmetry. As a consequence, its energy levels may be classified according to symmetry type. The symmetry types of the octahedral group are A_1 and A_2 (both nondegenerate), E (doubly degenerate), and T_1 and T_2 (both triply degenerate).

The classical version of the Hecht Hamiltonian is obtained by regarding $\mathbf{J}$ as a classical angular momentum with magnitude $J=(j+\frac{1}{2})\hbar$. Its time evolution is given by Euler's equation,

$$\dot{\mathbf{J}}=\boldsymbol{\omega}\times\mathbf{J},\quad \boldsymbol{\omega}=-\nabla H . \tag{2}$$

Euler's equation conserves the total angular momentum J^2, so that trajectories are confined to spheres in $\mathbf{J}$ space. It turns out that Eq. (2) may be cast in canonical form. The variables $q=\phi$ and $p=-J_z=-J\cos\theta$, where (θ,ϕ) are polar angles, are canonically conjugate. In terms of q and p, the Hecht Hamiltonian is given by

$$H=bp^4+b(\cos^4q+\sin^4q)(J^2-p^2)^2 . \tag{3}$$

[In Eq. (3) and in what follows, we drop the terms aJ^2 and $-3/5bJ^4$ as these have no effect on the dynamics.] The canonical equations of motion,

$$\dot{q}=\frac{\partial H}{\partial p},\quad \dot{p}=-\frac{\partial H}{\partial q} , \tag{4}$$

are then equivalent to Euler's equation. Equation (4) describes a system of one degree of freedom. Its phase space is spherical rather than Cartesian. Also, the Hamiltonian is not simply a sum of kinetic and potential terms. It is these facts which complicate the application of standard WKB methods.

Let us discuss the classical dynamics generated by the Hecht Hamiltonian. Trajectories are curves of constant energy. These are displayed in Fig. 1(a) in the (q,p) representation. The energy ranges between $E_{\min}=\frac{1}{3}bJ^4$ and $E_{\max}=bJ^4$. At the maximum and minimum energies there are six and eight stable fixed points, respectively. At $E=\frac{1}{2}bJ^4\equiv E_s$ there are 12 unstable fixed points. In physical terms the fixed points describe the uniform rotation of the molecule about a fixed axis. For $E_{\max}>E>E_s$ there are six periodic orbits encircling the energy maxima. Similarly, for $E_s>E>E_{\min}$, there are eight periodic orbits encircling the energy minima. These orbits describe the precession of the molecule about a stable axis of rotation. The sense of precession is indicated in Fig. 1(a): clockwise for $E>E_s$ and counterclockwise for $E<E_s$. Finally, at $E=E_s$ there are separatrices which join the unstable fixed points and separate the two kinds of periodic orbits.

One disadvantage of the (q,p) representation is that it obscures the symmetry of the dynamics. The octahedral rotations are rather complicated when expressed in terms of q and p. However, within the $\mathbf{J}$ representation [i.e., Eqs. (1) and (2)] it is easily shown that the periodic orbits at a given energy are mapped into each other by octahedral rotations. In particular, orbits at $E>E_s$ are invariant under a fourfold rotation about their centers, and orbits at $E<E_s$ are invariant under a threefold rotation about their centers. These features are readily apparent in the figures and discussion in I, as well as in Ref. 9.

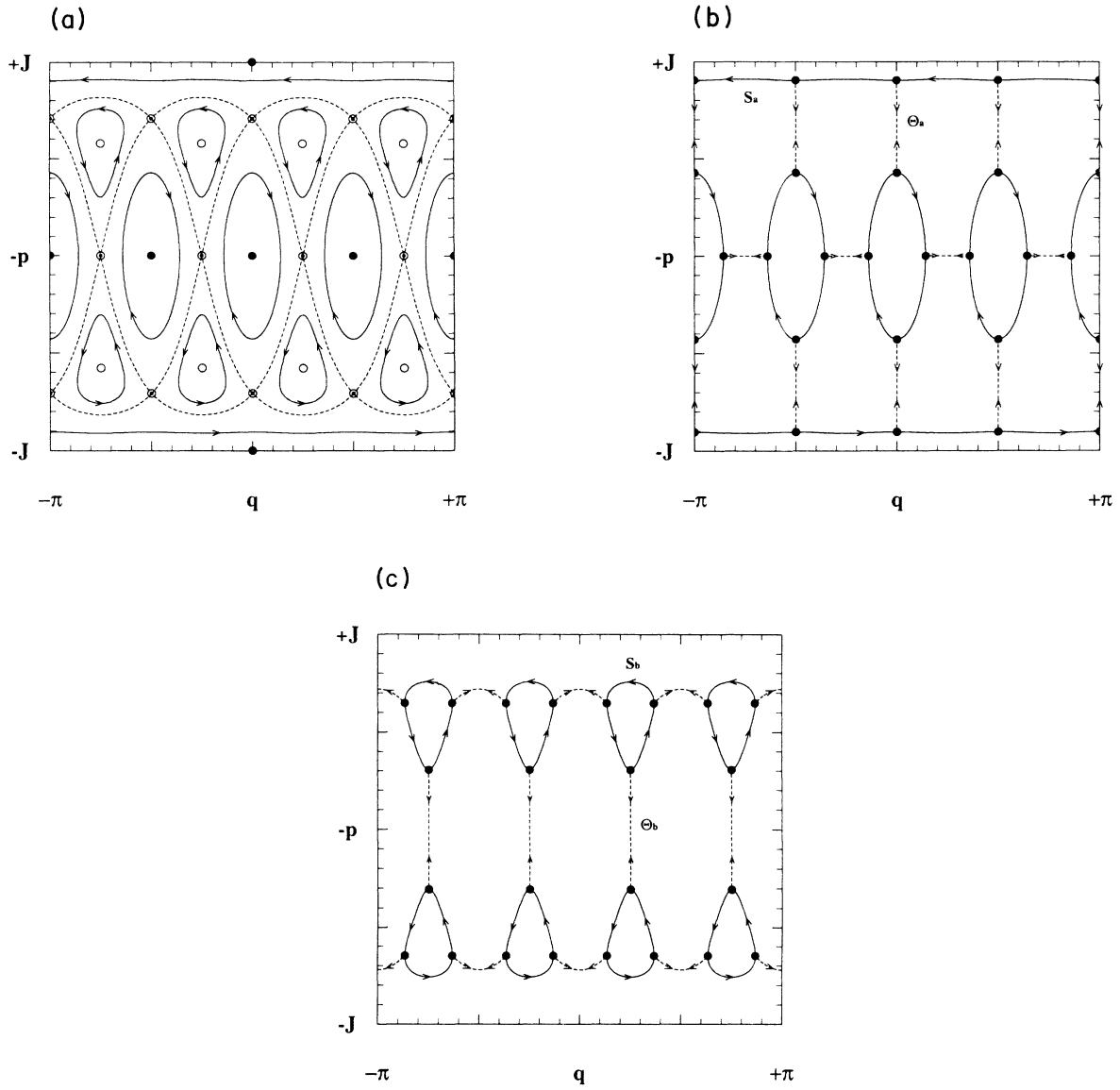

FIG. 1. Phase-space dynamics of the Hecht Hamiltonian. $q=\phi$ and $-p=J\cos\theta$, where (θ,ϕ) are polar angles on the angular momentum sphere and $J=j+\frac{1}{2}$. (a) Orbits above, at, and below the separatrix. The separatrix is the dotted orbit. Energy maxima are closed circles, saddle points are half-closed circles, and energy minima are open circles. (b) Periodic orbits above the separatrix. Tunneling orbits are dotted and nodes are closed circles. The orbits along which the classical and tunneling actions (S_a and Θ_a, respectively) are calculated are as indicated. (c) Periodic orbits below the separatrix. As in (b), tunneling orbits are dotted and nodes are closed circles. The orbits along which S_b and Θ_b are calculated are as indicated.

B. The complex periodic orbit sum

The discussion of the classical Hamiltonian already provides insight into the corresponding quantum spectrum. The Bohr-Sommerfeld quantization rule predicts energy levels at values of E for which the actions of periodic orbits are quantized. As there are either six or eight equivalent orbits at a given energy, one expects corresponding degeneracies in the quantum spectrum. In fact, these degeneracies are only approximate; the symmetry among classical orbits is broken at the quantum level by tunneling between the orbits. It is these tunneling effects which we would like to describe. Our calculation is based on periodic orbit theory, according to which the trace of the quantum-mechanical Green's function, $g(E)=\mathrm{Tr}[(E-H)^{-1}]$, is approximately expressed as a sum over classical periodic orbits with energy E and their repetitions, as follows:

$$g^{\mathrm{sc}}(E)=\sum_j F_j e^{i\Gamma_j} . \tag{5}$$

The j sum is taken over periodic orbits with energy E, and the amplitudes and phases F_j and Γ_j are determined

by the classical dynamics, and will be discussed presently. Energy levels are given by the poles of Eq. (5). To obtain tunneling effects, we include complex as well as real orbits in the sum. We will often refer to $g(E)$ simply as the Green's function. $g^{sc}(E)$ is its semiclassical approximation.

In I we discussed a prescription for the complex periodic orbit sum, hereinafter called the primitive prescription. We shall not review it in any detail. Instead we shall proceed directly to the new results and point out differences with the earlier treatment along the way. In what follows, we introduce a modified prescription for the complex periodic orbit sum, the uniform prescription. Applied to the double well, the uniform prescription leads to the familiar uniform results.[22] Here, we use it to derive uniform quantization conditions for the Hecht Hamiltonian.

The structure of the complex periodic orbits is shown in Figs. 1(b) and 1(c) for energies above and below the separatrix. Pairs of real periodic orbits (solid curves) are joined by tunneling orbits (dotted curves) along which either q or p is complex. Tunneling occurs at generalized turning points,or nodes (closed circles). For $E > E_s$ there are four nodes per real orbit; for $E < E_s$ there are three nodes per real orbit. We will call the portion of a real orbit between two neighboring nodes a classical segment.

A complex trajectory in the sum begins on a real orbit. Between nodes it acquires a phase e^{iA}, where A is the action along a classical segment. if $S = \oint p\, dq$ around the complete orbit, then

$$A_a = S_a/4, \quad A_b = S_b/3 . \tag{6}$$

(Here and in what follows, we use subscripts "a" or "b" to indicate that a quantity is evaluated at energies above or below the separatrix. When it is not necessary to make this distinction, we omit the subscripts.) A_a is one-fourth the action around an orbit above the separatrix; A_b is one-third the action of an orbit below the separatrix. There are some subtleties concerning the definition of S arising from the fact that the phase space is spherical. The canonical variables (q,p) are defined with respect to a polar axis, and S depends on whether or not the orbit encloses this axis. In Eq. (6), the polar axis is taken through the periodic orbit. Explicit formulas for S_a and S_b are given in Appendix A. When the trajectory reaches a node, it is either reflected or transmitted. Reflected trajectories continue along the real orbit and transmitted trajectories tunnel to another real orbit and continue from there. At each reflection the trajectory acquires an amplitude r, and at each transmission, an amplitude t. The quantities r and t are the WKB barrier reflection and transmission coefficients,[23] given by

$$r_a = \frac{e^{-i\delta}}{(1+e^{-2\Theta})^{1/2}}, \quad r_b = \frac{e^{i\delta}}{(1+e^{-2\Theta})^{1/2}},$$
$$t_a = \frac{-i(-1)^j e^{-\Theta} e^{-i\delta}}{(1+e^{-2\Theta})^{1/2}}, \quad t_b = \frac{i(-1)^j e^{-\Theta} e^{i\delta}}{(1+e^{-2\Theta})^{1/2}} . \tag{7}$$

In Eq. (7) Θ is the tunneling action $i\int p\, dq$ along a tunneling orbit. Explicit formulas for Θ above and below the separatrix are given in Appendix A; as defined, it is real and positive. The phase δ is given by[11,23]

$$\delta = \arg\Gamma\left[\frac{1}{2}+i\frac{\Theta}{\pi}\right] - \frac{\Theta}{\pi}\left[\ln\left|\frac{\Theta}{\pi}\right| - 1\right] . \tag{8}$$

The sign of δ in Eq. (7) corresponds to an overdense barrier for $E < E_s$ and an underdense barrier for $E > E_s$. The phases of r and t in Eq. (7) do not agree with the phases quoted in the references.[23] Their phases are chosen here to incorporate the Maslov index for the spherical phase space, and are discussed in I.

This prescription is to be contrasted with the primitive prescription, in which

$$r_a = 1, \quad r_b = 1 ,$$
$$t_a = -i(-1)^j e^{-\Theta}, \quad t_b = i(-1)^j e^{-\Theta} .$$

In the small tunneling, or large-Θ limit, the two prescriptions coincide. However, the uniform prescription has the important property of probability conservation;

$$|r|^2 + |t|^2 = 1 . \tag{9}$$

Also, because of the definite phase relation between r and t,

$$r^2 - t^2 = e^{\pm 2i\delta} . \tag{10}$$

As it turns out, an important consequence of Eqs. (9) and (10) is that the semiclassical Green's function has poles at real energies. The primitive prescription does not satisfy a relation like Eq. (9) or (10), and leads to a semiclassical Green's function with complex poles. (The complex part of the poles is small when the tunneling amplitude is small, and one obtains primitive quantization conditions by simply ignoring the complex part.) There is another difference between the uniform and primitive prescriptions. In the primitive prescription, we include trajectories which tunnel back and forth between nodes an arbitrary number of times before continuing along a real trajectory. In the uniform prescription, trajectories are allowed to tunnel only once between nodes. In effect, the reflection and transmission coefficients take into account the effects of multiple reflections within the barrier.

In order to carry out the complex periodic sum, we need a way to to parametrize the complex trajectories. The following scheme is convenient. Take n to be the number of times a trajectory is transmitted, and let a_i be the number of classical segments between the ith and $(i+1)$th transmission. It follows that $a_i - 1$ is the number of reflections between consecutive transmissions. (The coefficient a_n has a somewhat different meaning; it is the number classical segments between the last transmission and the trajectory's end. The number of reflections along this stretch is a_n and not $a_n - 1$, because there is an extra reflection at the trajectory's end as it closes on itself). The parameters (n,a_i), where $n \geq 0$, $a_i > 0$ for $i = 0,\ldots,n-1$ and $a_n \geq 0$ uniquely specify the complex trajectories. (We allow $a_n = 0$ to account for orbits which end immediately after their last transmission.) The amplitude and phase of the trajectory (n,a_i) is given by

$$r^{(a_0-1)+\cdots+(a_{n-1}-1)+a_n}t^n e^{i(a_0+\cdots+a_n)A} . \quad (11)$$

It is the product of the reflection and transmission coefficients and the semiclassical phases accumulated along the trajectory.

The complex periodic orbit sum is to be taken over closed trajectories. However, the trajectory (n,a_i) is, in general, not closed. Using geometric and group-theoretic arguments, we showed in I that the expression

$$\frac{1}{24}\sum_m d_m \chi_m(\omega^{a_0}\tau\omega^{a_1}\cdots\tau\omega^{a_n}) \quad (12)$$

is equal to 1 if (n,a_i) is closed, and vanishes otherwise. The sum in Eq. (12) is taken over irreducible representations of the octahedral group; $\chi_m(g)$ are the characters and d_m the dimensions of the representations. The group elements ω and τ are defined as follows:[20,24]

$$\begin{aligned}\omega_a &= R_y(\pi/2)R_z(\pi/2) ,\\ \omega_b &= R_z(-\pi/2) ,\\ \tau &= R_y(\pi/2)R_z(\pi) ,\end{aligned} \quad (13)$$

where the operation $R_e(\alpha)$ consists of a rotation about the $\hat{\mathbf{e}}$ axis by an angle α. Taken together, ω_a and τ generate the octahedral group, as do ω_b and τ.

To restrict the complex periodic orbit sum to closed trajectories, we sum over the parameters n and a_i, but then multiply the trajectory amplitudes Eq. (11) by Eq. (12). We obtain the following:

$$g^{sc}(E)=\sum_m \frac{d_m}{24}\sum_{n=0}^{\infty}\sum_{\substack{a_i=1\\0\le i<n}}^{\infty}\sum_{a_n=0}^{\infty}\chi_m(\omega^{a_0}\tau\omega^{a_1}\cdots\tau\omega^{a_n}) \times r^{-n}t^n(re^{iA})^{a_0+\cdots+a_n} . \quad (14)$$

The energy dependence of the right-hand side is contained in the action A and the reflection and transmission coefficients r and t.

In Eq. (14), if m is fixed instead of summed, the resulting expression contains poles at energy levels with symmetry m. This fact was discovered in I; the explanation for it is developed in Ref. 25. There it is shown that the sum over open trajectories can be interpreted as a sum over periodic orbits on a symmetry-reduced phase space. By appropriately weighting these orbits by group characters, one obtains an expression for the symmetry-projected density of states $g_m^{sc}(E)$, whose poles are energy levels with symmetry m. Let us fix m in Eq. (14). Also, let us replace $\chi(g)$ by $\mathrm{Tr}\underline{D}_m(g)$, where the matrix $\underline{D}_m(g)$ is the matrix representative of g. Using the representation property $\underline{D}_m(gg')=\underline{D}_m(g)\underline{D}_m(g')$, we obtain

$$g_m^{sc}(E)=\frac{d_m}{24}\sum_{n=0}^{\infty}\sum_{\substack{a_i=1\\0\le i<n}}^{\infty}\sum_{a_n=0}^{\infty} r^{-n}\mathrm{Tr}(\underline{\Omega}^{a_0}\underline{T}\,\underline{\Omega}^{a_1}\cdots\underline{T}\,\underline{\Omega}^{a_n}) ,$$

where $\underline{\Omega}=re^{iA}\underline{D}_m(\omega)$ and $\underline{T}=t\underline{D}_m(\tau)$. The sums over n and a_i are geometric series and are easily carried out. The result is

$$g_m^{sc}(E)=\frac{d_m}{24}\mathrm{Tr}\{[e^{-iA}\underline{D}_m^{\dagger}(\omega)-r\underline{I}_m-t\underline{D}_m(\tau)]^{-1} \times[e^{iA}\underline{D}_m(\omega)]\} . \quad (15)$$

In Eq. (15), $\underline{I}_m$ is the identity matrix of dimension d_m. The poles of $g_m^{sc}(E)$ occur when the matrix $e^{-iA}\underline{D}_m^{\dagger}(\omega)-r\underline{I}_m-t\underline{D}_m(\tau)$ is singular. This leads to the quantization condition

$$\det[(e^{-iA}\underline{D}_m^{\dagger}(\omega)-r\underline{I}_m-t\underline{D}_m(\tau)]=0 . \quad (16)$$

Note that each irreducible representation generates its own quantization condition.

The determinant in Eq. (16) may be expressed as a polynomial in e^{-iA} of degree d_m. (d_m is the dimension of the mth representation.) Its roots determine the semiclassical energy levels. For the energy levels to be real, the roots must have unit modulus. It is not obvious from Eq. (16) that this is the case, but it turns out, by virtue of Eqs. (9) and (10), to be so. A demonstration of this fact is given in Appendix C.

To obtain explicit expressions for the quantization conditions we need the matrix representatives $\underline{D}_m(\omega)$ and $\underline{D}_m(\tau)$. These are given in Appendix B. In Appendix C it is shown that the complex quantization condition Eq. (16) can be reduced to a real quantization condition,

$$Q_m(E)=0 . \quad (17)$$

Above the separatrix, the quantization functions Q_m are given by

$$\begin{aligned}Q_{A_1} &= \sin\left[\frac{I_a-\beta}{2}\right] ,\\ Q_{A_2} &= \cos\left[\frac{I_a+\beta}{2}\right] ,\\ Q_E &= \sin I_a+\tfrac{1}{2}\sin\beta ,\\ Q_{T_1} &= \cos I_a+\cot\left[\frac{I_a+\beta}{2}\right]\sin I_a-\cos\beta ,\\ Q_{T_2} &= -\cos I_a+\tan\left[\frac{I_a-\beta}{2}\right]\sin I_a-\cos\beta, \quad E>E_s ,\end{aligned} \quad (18a)$$

where

$$I_a=A_a-\delta, \quad \beta=(-1)^j\tan^{-1}(e^{-\Theta}) . \quad (18b)$$

Below the separatrix, they are given by

$$Q_{A_1}=-\sigma_1\sin\left[\frac{I_b-\beta}{2}\right],$$

$$Q_{A_2}=-\sigma_2\sin\left[\frac{I_b+\beta}{2}\right],$$

$$Q_E=(-1)^j(\cos I_b+\tfrac{1}{2}\cos\beta), \tag{18c}$$

$$Q_{T_1}=\sigma_1\left[\sin I_b+\tan\left[\frac{I_b+\beta}{2}\right]\cos I_b-\sin\beta\right],$$

$$Q_{T_2}=\sigma_2\left[\sin I_b+\tan\left[\frac{I_b-\beta}{2}\right]\sin I_b+\sin\beta\right],\quad E<E_s,$$

where

$$I_b=-A_b-\delta,\quad \beta=(-1)^j\tan^{-1}(e^{-\Theta}),$$

$$\sigma_1=\begin{cases}-1, & j \bmod 4=1,2\\ 1, & j \bmod 4=3,0\end{cases} \tag{18d}$$

$$\sigma_2=\begin{cases}-1, & j \bmod 4=0,1\\ 1, & j \bmod 4=2,3\end{cases}.$$

The overall sign factors which appear in Eq. (18c), σ_1 and σ_2, are irrelevant as far as the quantization condition Eq. (17) is concerned. However, they are needed to make the quantization functions continuous as E_s, as will be explained in Sec. II D.

The quantization conditions, Eqs. (16)–(18) represent the principle result of this paper. The formulas depend on the actions of the classically allowed and forbidden trajectories as well as the generators ω and τ of the symmetry group. The preceding analysis may be applied to other symmetry groups. In what follows, we discuss some analytic results which follow from Eqs. (16)–(18).

C. Small tunneling limit

Let us examine the uniform quantization conditions in the small tunneling, or large-Θ limit. This limit is appropriate for energies far from the separatrix. First, let us take $\beta=e^{-\Theta}$ to be identically zero. Then Eqs. (18a) and (18c) simplify to give a single quantization condition irrespective of symmetry type,

$$S(E_k)-\delta=2\pi k. \tag{19}$$

Except for δ, the shift in action, Eq. (19) is just the usual Einstein-Brillouin-Keller (EBK) quantization condition

$$S=\oint p\,dq=-(j+\tfrac{1}{2})\oint\cos\theta\,d\phi=2\pi k$$

(Ref. 26). The EBK energy levels are either sixfold or eightfold degenerate according to whether $E>E_s$ or $E<E_s$. In fact, the shift in action δ is not significant for large Θ. The EBK quantization may be derived from an asymptotic expansion in powers of $1/j$. It contains terms of order j and order 1, but neglects terms of order $1/j$ and higher. From Eq. (8), one determines that

$$\delta(\Theta)\to\frac{1}{24}\frac{\pi}{\Theta}$$

for large Θ. As Θ is of order j, δ is of order $1/j$. It is a correction of higher order than the asymptotic expansion warrants.

Next, we expand $Q_m(E)$ about the EBK energy E_k, regarding $e^{-\Theta}$ as small but not vanishing, and taking $E-E_k$ to be of order $e^{-\Theta}$. Note that $S'(E)=T$, where T is the classical period. The six- and eightfold degeneracies are partially split, leaving nearly degenerate clusters of levels. The levels in the clusters have definite symmetry type. The splitting patterns depend on k, specifically on k mod4 for $E>E_s$, and k mod3 for $E<E_s$. Letting $\Delta=(-1)^je^{-\Theta}$, we obtain the splittings

$$\begin{aligned}&\epsilon_E=-2\Delta,\quad \epsilon_{T_1}=0,\quad \epsilon_{A_1}=4\Delta;\quad k \bmod 4=0\\ &\epsilon_{T_1}=-2\Delta,\quad \epsilon_{T_2}=2\Delta;\quad k \bmod 4=1\\ &\epsilon_{A_2}=-4\Delta,\quad \epsilon_{T_2}=0,\quad \epsilon_E=2\Delta;\quad k \bmod 4=2\\ &\epsilon_{T_1}=-2\Delta,\quad \epsilon_{T_2}=2\Delta;\quad k \bmod 4=3\end{aligned} \tag{20a}$$

for $E>E_s$ and for $E<E_s$,

$$\epsilon_{A_1}=-3\Delta,\quad \epsilon_{T_1}=-\Delta,\quad \epsilon_{T_2}=\Delta,\quad \epsilon_{A_2}=3\Delta;\quad k \bmod 3=0$$

$$\epsilon_{T_2}=-2\Delta,\quad \epsilon_E=0,\quad \epsilon_{T_1}=2\Delta;\quad k \bmod 3=1 \tag{20b}$$

$$\epsilon_{T_2}=-2\Delta,\quad \epsilon_E=0,\quad \epsilon_{T_1}=2\Delta;\quad k \bmod 3=2.$$

In Eq. (20), ϵ_m is the energy shift relative to E_k of an energy level with symmetry m. As an example, suppose $E_k>E_s$ and k mod4$=0$. Then there is an A_1 level with energy $E_k=4\Delta$, a T_1 level with energy E_k, and an E level with energy $E_k-2\Delta$. Note that the number of levels in the cluster, counting degeneracies, is six. It is straightforward to verify that Eq. (20) is equivalent to the results obtained in I and to those of Harter and Patterson.[8,9]

D. Continuity at the separatrix

The real power of the uniform quantization conditions is near the separatrix. There the tunneling amplitude $e^{-\Theta}$ is no longer small, and the primitive quantization conditions Eq. (20) are no longer valid. The uniform quantization conditions, however, remain accurate near the separatrix, as the numerical results demonstrate. Here we show that the functions $Q_m(E)$ are continuous at $E=E_s$.

The tunneling action vanishes at the separatrix. It follows that

$$r=t=\frac{1}{\sqrt{2}},\quad \Theta=\delta=0 \tag{21}$$

at $E=E_s$. There exists as well a relation between the actions $A_a(E_s)$ and $A_b(E_s)$. It is straightforward to show that the area of phase space above the separatrix, denoted here by Ω_a, is given by $6[2\pi(j+\frac{1}{2})-S_a(E_s)]$. Similarly, the area of phase space below the separatrix Ω_b is given by $8[2\pi(j+\frac{1}{2})+S_b(E_s)]$. [The area is the integral $(j+\frac{1}{2})\int\int\sin\theta\,d\theta\,d\phi$, and the results above follow from

Stoke's theorem.] The total area of phase space Ω is $4\pi(j+\frac{1}{2})$. From $\Omega_a+\Omega_b=\Omega$ and Eq. (6), it follows that

$$A_a - A_b = (j+\tfrac{1}{2})\pi \ . \tag{22}$$

If we substitute Eqs. (21) and (22) into Eqs. (18a) and (18c), it is straightforward to show that $Q_m(E)$ is continuous at $E=E_s$. The sign factors σ_1 and σ_2 in Eq. (18c) are needed to establish this result.

The quantization functions are not smooth at the separatrix, however, because the derivatives of both S and Θ have logarithmic singularities at $E=E_s$. But with a suitable analytic continuation of S and Θ around the branch point at $E=E_s$ in the complex energy plane, we can derive Eq.(18c) from Eq. (18a). Let us sketch this result. By choosing branch cuts in p appropriately, we can analytically continue A_a to energies below the separatrix. Its continuation is related to A_b as follows:

$$A_a = A_b + (j+\tfrac{1}{2})\pi \ . \tag{23}$$

Θ_a may be analytically continued below the separatrix so that

$$\Theta_a = -\Theta_b \ . \tag{24}$$

Above the separatrix the uniform quantization condition Eq. (16) is given by

$$\det[(e^{-iA_a}\underline{D}^{\dagger}_m(\omega_a) - r_a\underline{I}_m - t_a\underline{D}_m(\tau)] = 0 \ . \tag{25}$$

Let us continue it below the separatrix. From Eq. (24) and Eqs. (7) and (8) it follows that

$$\begin{aligned} &r_a = -i(-1)^j t_b, \quad t_a = -i(-1)^j r_b \ , \\ &\delta(\Theta_a) = -\delta(\Theta_b) \ , \end{aligned} \tag{26}$$

where r_b and t_b are the reflection and transmission coefficients below the separatrix, and r_a and t_a are the same coefficients analytically continued from above. There is also a relation between the group element ω above and below the separatrix. From Eq. (13), it follows that

$$\omega_a = \tau\omega_b \ . \tag{27}$$

Substituting Eqs. (23), (26), and (27) into Eq. (25) we obtain

$$\begin{aligned} \det[&-i(-1)^j e^{-iA_b}\underline{D}^{\dagger}_m(\omega_b)\underline{D}^{\dagger}_m(\tau) \\ &-i(-1)^j t_b\underline{I} - i(1)^j r_b\underline{D}_m(\tau)] = 0 \ . \end{aligned} \tag{28}$$

Let us multiply the determinant in Eq. (28) by $\det[i(-1)^j\underline{D}_m(\tau)]$. From Eq. (13), $\tau^2=I$, so that $[\underline{D}_m(\tau)]^2=\underline{I}_m$. Equation (28) becomes

$$\det[(e^{-iA_b}\underline{D}^{\dagger}_m(\omega_b) - r_b\underline{I}_m - t_b\underline{D}_m(\tau)] = 0 \ . \tag{29}$$

This is precisely the quantization condition below the separatrix.

E. Periodicity in symmetry types

Fox *et al.* discovered a remarkable periodicity in the spectrum of the Hecht Hamiltonian.[5] With increasing energy, the eigenvalues occur in one of the following sequences, depending on the parity of j:

$$\begin{aligned} &(A_1, T_1, T_2, A_2, T_2, E, T_1, T_2, E, T_1), \quad j \text{ even} \\ &(T_1, E, T_2, T_1, E, T_2, A_2, T_2, T_1, A_1), \quad j \text{ odd} \ . \end{aligned} \tag{30}$$

These sequences can be deduced from the small tunneling limit of the quantization conditions, Eq. (20). In this limit they have been beautifully explained by Harter and Patterson, who show that the nearly degenerate semiclassical eigenstates transform according to induced representations of the octahedral group. Equation (30) then follows from the Frobenius reciprocity theorem. However, the analysis of Harter and Patterson breaks down near the separatrix. Surprisingly, the eigenvalue sequences continue uninterrupted through the separatrix. In this section we derive this result from the uniform quantization conditions.

To begin, we scale the tunneling action Θ in Eq. (18),

$$\Theta \to s\Theta, \quad 0 \le s \le 1 \ . \tag{31}$$

We obtain thereby a family of quantization functions $Q_m(E;s)=0$ and their roots $E_n(s)$, parametrized by the scaling factor s. With $s=1$ we recover the original quantization conditions. Consider instead the case $s=0$. This is sort of the opposite of the small tunneling limit; the magnitudes of the reflection and transmission coefficients are both $1/\sqrt{2}$, $\beta=(-1)^j\pi/4$ and $\delta=0$, and Eq. (18) simplifies considerably. Above the separatrix,

$$\begin{aligned} Q_{A_1} &= \sin\left[\frac{A_a-(-1)^j\pi/4}{2}\right] , \\ Q_{A_2} &= \cos\left[\frac{A_a+(-1)^j\pi/4}{2}\right] , \\ Q_E &= \sin A_a + \frac{(-1)^j\sqrt{2}}{4} \ , \\ Q_{T_1} &= \cos A_a + \cot\left[\frac{A_a+(-1)^j\pi/4}{2}\right]\sin A_a - \frac{\sqrt{2}}{2} \ , \\ Q_{T_2} &= -\cos A_a + \tan\left[\frac{A_a-(-1)^j\pi/4}{2}\right]\sin A_a - \frac{\sqrt{2}}{2} \ . \end{aligned} \tag{32}$$

For $s=0$, the quantization functions below the separatrix are obtained from those above by the substitution $A_b = A_a - (j+\frac{1}{2})\pi$. Therefore the entire spectrum may be obtained from Eq. (32). The functions in Eq. (32) are periodic in A_a. This explains why the symmetry labels appear in a periodic sequence, at least for $s=0$. Let us determine the order in which they occur. For A_1 and A_2 symmetries we can write down quantized actions; these are $A_a=(2n+\frac{1}{4})\pi$ and $A_a=(2n+\frac{3}{4})\pi$ for j even, and $A_a=(2n+\frac{7}{4})\pi$ and $A_a=(2n+\frac{5}{4})\pi$ for j odd. For the other symmetry classes the quantized actions must be calculated numerically. The results are given in Table I over

TABLE I. Roots of quantization functions for $\Theta=0$, $E>E_s$.

j even		j odd	
m	A_a	m	A_a
A_1	$\pi/4$	T_1	0.10
T_1	1.38	E	0.36
T_2	1.76	T_2	1.08
A_2	$3\pi/4$	T_1	2.07
T_2	3.24	E	2.78
E	3.50	T_2	3.04
T_1	4.22	A_2	$5\pi/4$
T_2	5.21	T_2	4.52
E	5.92	T_1	4.90
T_1	6.18	A_1	$7\pi/4$

the range $0\leq A_a\leq 2\pi$; they show that the quantization functions produce the sequences of Eq. (30).

Next we continuously increase s to its original value $s=1$. The roots of $Q_m(E;s)$ shift along the energy axis. However, they cannot cross the separatrix. Because Θ vanishes at the separatrix, $s\Theta(E_s)=0$ regardless of s, and $Q_m(E_s;s)$ is constant. Thus the roots of $Q_m(E;s)$ are pinned on either side E_s. The final step in the argument is to demonstrate that with increasing s, the roots of the different quantization functions cannot cross each other. The calculation is straightforward but somewhat tedious, and is given in Appendix D. Since the sequences of Eq. (30) are produced when $s=0$ and the ordering of the eigenvalues does not change with s, it follows that Eq. (30) is produced by the original quantization formulas, Eq. (18).

III. NUMERICAL RESULTS

Quantum-mechanical, uniform, and primitive eigenvalues of the Hecht Hamiltonian were calculated for angular momentum $j=88$. [The explicit form of the primitive quantization conditions is obtained by taking $\delta=0$ in Eq. (20).] Away from the separatrix, the energy levels coalesce into nearly degenerate clusters containing eight levels for $E<E_s$, and six levels for $E>E_s$. In this regime one distinguishes two splitting scales: the fine splitting between adjacent clusters and the superfine splitting between levels within a cluster. The fine splitting is the energy difference between consecutive Bohr-Sommerfeld energy levels and is given approximately by the classical frequency $\omega=2\pi/T$. ω scales with j as j^3. The superfine splitting is produced by tunneling and is proportional to $e^{-\Theta}/T$. Θ scales linearly with j, so the superfine splitting becomes exponentially small with j.

This separation of scales breaks down at the separatrix. There Θ approaches zero, and the fine and superfine splittings are of the same order. In this regime one expects uniform quantization to be superior to the primitive quantization. In Table II, we give the energy splittings ΔE_n near the separatrix between consecutive nondegenerate energy levels, defined by

$$\Delta E_n=E_n-E_{n-1}\ , \tag{33}$$

according to the three quantization schemes. The quantum number n is counted upwards from the bottom of the spectrum. The separatrix lies between $n=64$ and 65. The values of n are not consecutive because some energy levels (those with symmetry E, T_1, or T_2) are exactly degenerate, and the splitting between them is trivially zero. From Table II, the uniform splittings are accurate to three or four decimal places, while errors in the primitive splittings occur in the first or second decimal place. For example, at $n=61$ the uniform error is between 0.1% and 0.2% while the primitive error is about 30%.

TABLE II. Energy splittings near separatrix (10^{-4} cm^{-1}).

n	$\Delta E_n(Q)$[a]	$\Delta E_n(U)$[b]	$\Delta E_n(P)$[c]
49	17.170	17.174	17.341
52	1.044	1.040	1.128
54	0.981	0.977	1.128
57	10.485	10.496	9.245
58	2.211	2.205	3.006
61	2.224	2.221	3.006
64	4.463	4.450	3.006
65	4.746	4.754	3.844
68	1.306	1.307	1.996
70	9.087	9.072	8.842
73	1.784	1.788	1.817
76	12.743	12.728	12.927
78	0.301	0.301	0.312
81	0.563	0.564	0.625
82	15.431	15.418	15.496
85	0.169	0.169	0.177

[a] Q denotes quantum-mechanical eigenvalues.
[b] U denotes uniform semiclassical quantization.
[c] P denotes primitive semiclassical quantization.

From the numerical results it is evident that near the separatrix the order of magnitude of ΔE_n remains the same from one level to the next. As we leave the separatrix, the disparate scales of the fine and superfine splittings manifest themselves. Compare, for example, $\Delta E_{76}=12.743$ and $\Delta E_{78}=0.301$. E_{78} and E_{77} belong to the same cluster; E_{76} and E_{75} do not.

Far from the separatrix the primitive and uniform quantization conditions give comparable results. They must, because to within terms second order in $e^{-\Theta}$, the two quantizations conditions differ only by the phase shift δ which appears in Eq. (19). As explained in Sec. II C, this correction is only significant near the separatrix. A comparison of uniform and primitive quantization throughout the spectrum may be found in Ref. 27; the uniform results tend to be a bit better. A comparison between primitive and quantum results was given by Harter and Patterson.[9]

IV. CONCLUSION

Periodic orbit theory provides uniform semiclassical quantization conditions for a tunneling system with octahedral symmetry, namely the rotational dynamics of SF_6. The quantization conditions depend on the actions of the classically allowed and forbidden orbits as well as the generators of the symmetry group. A separate quantiza-

tion condition for each symmetry class is obtained. Together these account for a previously observed periodicity in the eigenvalue symmetry labels. The uniform quantization conditions are shown to agree with previously obtained results in the small tunneling limit, and to provide significantly improved accuracy near the classical separatrix. The methods used here may be applied to other tunneling systems with symmetry, such as the rotational dynamics of icosahedrally symmetric molecules.[28] The role of complex periodic orbits in periodic orbit theory deserves further investigation, particular in higher-dimensional systems. One hopes that such investigation will lead to a theory of multidimensional tunneling.

ACKNOWLEDGMENTS

This work was supported by the Director, Office of Energy Research, Office of Basic Energy Sciences Research, Engineering and Geoscience Division of the U.S. Department of Energy under Contract No. DE-AC03-76SF00098 and by the National Science Foundation under Grant No. NSF-PYI-84-51276.

APPENDIX A: ACTION INTEGRALS

We provide explicit formulas for the action integrals S and Θ. First, some general remarks. The action is defined by $S=\oint p\,dq=-\oint J_z d\phi$, where $J_z=(j+\frac{1}{2})\cos\theta$. The integral is taken around a periodic orbit and the sense of the integral is the sense of the orbit as determined by the equations of motion. J_z is determined by the equation $H(J_z,\phi)=E$. It turns out that the value of S depends on the choice of $\hat{\mathbf{z}}$, the axis of quantization. To illustrate this, assume for the moment that the orbit is clockwise (with respect to an outward normal on the angular momentum sphere.) Take the positive $\hat{\mathbf{z}}$ axis through the orbit, and choose another axis $\hat{\mathbf{z}}'$ outside the orbit. One can show that $S=S'+2\pi(j+\frac{1}{2})$, where S and S' are the actions referred to the quantization axes $\hat{\mathbf{z}}$ and $\hat{\mathbf{z}}'$, respectively. If instead the orbit is counterclockwise, then $S=S'-2\pi(j+\frac{1}{2})$. For both $E<E_s$ and $E>E_s$ the axis of quantization is chosen through one of the periodic orbits. It is therefore different in each case.

Define

$$J_z^{\pm}(\phi,E)=(j+\tfrac{1}{2})\left[\frac{t(\phi)\pm\sqrt{\epsilon-(1-\epsilon)t(\phi)}}{1+t(\phi)}\right]^{1/2},$$

$$t(\phi)=\cos^4\phi+\sin^4\phi=\frac{3+\cos4\phi}{4}. \tag{A1}$$

$\epsilon=E/\beta$ in the above. Then

$$S_a(E)=\int_0^{2\pi}J_z^{+}d\phi, \tag{A2}$$

$$S_b(E)=\int_{\phi_0}^{\pi/2-\phi_0}(J_z^{+}-J_z^{-})d\phi-2\pi(j+\tfrac{1}{2}), \tag{A3}$$

where

$$\cos4\phi_0=\frac{7\epsilon-3}{1-\epsilon}.$$

In Eq. (A2) ϕ_0 is taken between 0 and $\pi/4$. The orbits around which the integrals are taken are indicated in Figs. 1(b) and 1(c).

The tunneling integrals are defined as follows:

$$\Theta_a=-i\int_{\phi_0}^{\pi/2-\phi_0}J_z^{-}d\phi, \tag{A4}$$

where $\cos4\phi_0=4\epsilon-3$. ϕ_0 is taken between 0 and $\pi/4$. J_z^{-} is pure imaginary, and the branch cuts in Eq. (A1) are chosen so that $\mathrm{Im}J_z^{-}>0$,

$$\Theta_b=-2i\int_{\pi/4}^{\pi/4+i\phi_0}J_z^{-}d\phi, \tag{A5}$$

where $\cosh4\phi_0=3-4\epsilon$. ϕ makes an excursion into the complex plane, and $d\phi$ is positive imaginary along the contour. The paths of integration for Eqs. (A4) and (A5) are indicated in Figs. 1(b) and 1(c).

APPENDIX B: IRREDUCIBLE REPRESENTATIONS

We give matrix representatives of the group elements ω and τ defined in Eq. (13). The representatives of ω_b can be obtained from those of ω_a and τ from the relation $\underline{D}_m(\omega_b)=\underline{D}_m(\tau)\underline{D}_m(\omega_a)$. [Cf. Eq. (27)] The one-dimensional representatives are $\underline{D}_{A_1}(\omega_a)=\underline{D}_{A_1}(\tau)=\underline{1}$ and $\underline{D}_{A_2}(\omega_a)=\underline{D}_{A_2}(\tau)=-\underline{1}$. The E and T_1 representatives are

$$\underline{D}_E(\omega_a)=\begin{bmatrix}1&0\\0&-1\end{bmatrix},$$

$$\underline{D}_E(\tau)=\tfrac{1}{2}\begin{bmatrix}-1&-\sqrt{3}i\\\sqrt{3}i&1\end{bmatrix},$$

$$\underline{D}_{T_1}(\omega_a)=\begin{bmatrix}0&1&0\\-1&0&0\\0&0&1\end{bmatrix}, \tag{B1}$$

$$\underline{D}_{T_1}(\tau)=\begin{bmatrix}0&0&1\\0&-1&0\\1&0&0\end{bmatrix}.$$

The T_2 representatives may be obtained from the relation $\underline{D}_{T_2}(g)=\underline{D}_{A_2}(g)\underline{D}_{T_1}(g)$, where g is any group element.

APPENDIX C: CALCULATION OF QUANTIZATION FUNCTIONS

We show that the roots of the complex quantization condition Eq. (16) are real and then derive the real quantization conditions, Eqs. (17) and (18). For the sake of brevity we consider a single representative case, namely the case of T_1 symmetry for $E>E_s$. Substituting Eq. (B1) for the matrix representatives and Eq. (7) for r and t into Eq. (16), we obtain the following explicit quantization condition:

$$z^3-(\cos\beta)z^2+(\cos\beta)e^{i\beta}z-e^{i\beta}=0, \tag{C1}$$

where $z=e^{-i(A-\delta)}$ and $\beta=(-1)^j\tan^{-1}e^{-\Theta}$. In deriving Eq. (C1) we have made use of Eq. (10). The left-hand side of Eq. (C1) is a cubic polynomial in z. For the quantiza-

tion condition to have real solutions, its roots must be phase factors. Let us try to find roots of the form $e^{i\alpha_1}, e^{i\alpha_2}, e^{i\alpha_3}$, where α_i is real. The necessary and sufficient conditions are that

$$e^{i(\alpha_1+\alpha_2+\alpha_3)}=e^{i\beta}\ , \tag{C2a}$$

$$e^{i(\alpha_1+\alpha_2)}+e^{i(\alpha_2+\alpha_3)}+e^{i(\alpha_3+\alpha_2)}=(\cos\beta)e^{i\beta}\ , \tag{C2b}$$

$$e^{i\alpha_1}+e^{i\alpha_2}+e^{i\alpha_3}=\cos\beta\ . \tag{C2c}$$

Equations (C2) constitute three complex equations in three real unknowns; one would not expect solutions to exist. However, one readily sees that the second equation can be obtained from the first and the third, and that the remaining equations are equivalent to the following three real equations:

$$\alpha_1+\alpha_2+\alpha_3=2\pi k+\beta\ , \tag{C3a}$$

$$\cos\alpha_1+\cos\alpha_2+\cos\alpha_3=\cos\beta\ , \tag{C3b}$$

$$\sin\alpha_1+\sin\alpha_2+\sin\alpha_3=0\ . \tag{C3c}$$

Let us eliminate α_2 and α_3 in favor of α_1. From Eq. (C3b) one has

$$\cos\alpha_1=\cos\beta-2\cos\frac{\alpha_2-\alpha_3}{2}\cos\frac{\alpha_2+\alpha_3}{2}\ . \tag{C4}$$

From Eq. (C3c) follows

$$2\cos\frac{\alpha_2-\alpha_3}{2}=-\sin\alpha_1\csc\frac{\alpha_2+\alpha_3}{2}\ . \tag{C5}$$

Substituting Eq. (C4) into Eq. (C5) and using $\alpha_2+\alpha_3=\beta-\alpha_1-2\pi k$ from Eq. (C3a), we obtain

$$\cos\alpha_1=\cos\beta+\sin\alpha_1\cot\frac{\beta-\alpha_1}{2}\ . \tag{C6}$$

This is precisely the quantization condition $Q_{T_1}(E)=0$ for $E>E_s$.

APPENDIX D: NONCROSSING PROPERTY

In Sec. II E we introduced a scaling of the tunneling action $\Theta\rightarrow s\Theta$ and claimed that the roots of the scaled quantization functions $Q_m(E,s)$ cannot cross. Let us demonstrate this result for a representative case, namely $m=E$, $m'=T_1$, and $E>E_s$. Suppose that

$$Q_E(E,s)=Q_{T_1}(E,s)=0\ . \tag{D1}$$

It is simplest to proceed from the complex quantization condition Eq. (16). Substituting Eqs. (7), (16), and (B1) into Eq. (D1) we obtain

$$z^2-i(\sin\beta)z-1=0 \quad \text{for } E \tag{D2a}$$

$$z^3-(\cos\beta)z^2+(\cos\beta)e^{i\beta}z-e^{i\beta}=0 \quad \text{for } T_1 \tag{D2b}$$

where $z=e^{-iA-\delta}$ and $\beta=(-1)^j\tan^{-1}(e^{-s\Theta})$. Multiplying the first equation by z and subtracting from it the second, we obtain

$$e^{-i\beta}z^2-(e^{i\beta}\cos\beta+1)z+e^{i\beta}=0\ . \tag{D3}$$

Next we multiply Eq. (D2a) by $e^{-i\beta}$ and subtract it from Eq. (D3). With some manipulation we obtain

$$(\cos^2\beta)z=\cos\beta\ . \tag{D4}$$

Since z has unit modulus, the only possible solutions are $\cos\beta=0$ and ±1. But $\cos\beta=(1+e^{-2s\Theta})^{-1/2}$, so there are in fact no solutions of Eq. (D1).

[1] K. W. Ford and J. A. Wheeler, Ann. Phys. (N.Y.) **7**, 259 (1959); **297**, (1959); W. H. Miller, J. Chem. Phys. **48**, 1651 (1968).

[2] C. W. Patterson, R. S. McDowell, N. G. Nereson, B. J. Krohn, J. S. Wells, and F. R. Peterson, J. Mol. Spectrosc. **91**, 416 (1982); K. C. Kim, W. B. Person, D. Seitz, and B. J. Krohn, *ibid.* **76**, 322 (1979); A. S. Pine and A. G. Robiette, *ibid.* **80**, 388 (1980); J. Bordé and Ch. J. Bordé, Chem. Phys. **71**, 417 (1982).

[3] J. Bordé, Ch. J. Bordé, C. Salomon, A. Van Lerberghe, M. Ouhayoun, and C. D. Cantrell, Phys. Rev. Lett. **45**, 14 (1980).

[4] K. T. Hecht, J. Mol. Spectrosc. **5**, 355 (1960).

[5] A. J. Dorney and J. K. G. Watson, J. Mol. Spectrosc. **42**, 135 (1972).

[6] K. Fox, H. W. Galbraith, B. J. Krohn, and J. D. Louck, Phys. Rev. A **15**, 1363 (1977).

[7] W. G. Harter and C. W. Patterson, Phys. Rev. Lett. **38**, 224 (1977).

[8] W. G. Harter and C. W. Patterson, J. Chem. Phys. **66**, 4872 (1977); **66**, 4886 (1977).

[9] W. G. Harter and C. W. Patterson, J. Chem. Phys. **80**, 4241 (1984).

[10] G. W. King, J. Chem. Phys. **15**, 820 (1947); R. M. Hainer, P. C. Cross, and G. W. King, *ibid.* **17**, 826 (1949); S. D. Augustin and W. H. Miller, *ibid.* **61**, 3155 (1974).

[11] S. M. Colwell, N. C. Handy, and W. H. Miller, J. Chem. Phys. **68**, 745 (1978).

[12] M. C. Gutzwiller, J. Math. Phys. **8**, 1979 (1967); **10**, 1004 (1969); **11**, 1791 (1970); **12**, 343 (1971).

[13] R. Balian and C. Bloch, Ann. Phys. (N.Y.) **60**, 401 (1970); **64**, 271 (1971); **69**, 76 (1972); **63**, 592 (1971); **85**, 514 (1974).

[14] M. V. Berry, in *Semiclassical Mechanics of Regular and Irregular Motion,* Proceedings of the Les Houches Summer School Session XXXVI, Les Houches, 1981, edited by G. Iooss, R. H. G. Hellman, and R. Stora (North-Holland, Amsterdam, 1983), p. 171; M. V. Berry and M. Tabor, Proc. R. Soc. London Ser. A **349**, 101 (1976); J. Phys. A **10**, 373 (1977).

[15] W. H. Miller, J. Phys. Chem. **83**, 960 (1979).

[16] R. Balian, G. Parisi, and A. Voros, in *Feynman Path Integrals,* Vol. 106 of *Lecture Notes in Physics,* edited by S. Alberverio, (Springer-Verlag, New York, 1979), p. 337.

[17] A. Voros, Ann. Inst. Henri Poincaré **39**, 211 (1983).

[18] D. M. Brink and U. Smilansky, Nucl. Phys. A **405**, 301 (1983).

[19] B. A. Anderson, Ph.D. dissertation, University of Texas at Austin, 1986.

[20] J. M. Robbins, S. C. Creagh, and R. G. Littlejohn, Phys. Rev. A **39**, 2838 (1989).

[21]C. W. Patterson, B. J. Krohn, and A. S. Pine, J. Mol. Spectrosc. **88**, 133 (1981); C. W. Patterson, F. Herlemont, M. Azizi, and J. Lemaire, *ibid.* **108**, 31 (1984).
[22]S. C. Creagh and R. G. Littlejohn (unpublished).
[23]M. V. Berry and K. E. Mount, Rep. Prog. Phys. **35**, 316 (1972).
[24]In fact, the definitions of ω and τ for $E < E_s$ are not the same as those given in Ref. 20, but are related to them by a conjugation. The expression in Eq. (12) is invariant under conjugation of ω and τ.
[25]J. M. Robbins, Phys. Rev. A **40**, 2128 (1989).
[26]I. Percival, Adv. Chem. Phys. **36**, 1 (1977).
[27]J. M. Robbins, Ph.D. thesis, University of California, Berkeley, 1989.
[28]W. G. Harter and D. E. Weeks, J. Chem. Phys. **90**, 4727 (1989); D. E. Weeks and W. G. Harter, *ibid.* **90**, 4744 (1989).